

# An Approach for the Development of ImmunoChip for the Detection of Celiac Disease based on Anti-Gliadin Antibodies Quantification

Shagun Gupta<sup>1</sup>, Ankur Kaushal<sup>1</sup>, Deepak Kala<sup>2</sup>, Adesh K. Saini<sup>1</sup>, Reena V. Saini<sup>1</sup>, Ashok Kumar<sup>3,\*</sup>, Dinesh Kumar<sup>4,\*</sup>

<sup>1</sup> Department of Biotechnology, Maharishi Markandeshwar University, Mullana, Ambala, 134003, India; shagun22\_88@yahoo.com (S.G.); ankur.biotech85@gmail.com (A.K.); sainiade@gmail.com (A.K.S.); reenavohra10@gmail.com (R.V.S)

<sup>2</sup> Department of Biotechnology Engineering and Food Technology, Chandigarh University, Mohali, 140413, India; deepakbiotech90cu@gmail.com (D.K.)

<sup>3</sup> CSIR-Institute of Genomics and Integrative Biology, Mall Road, Delhi-110007, India; ashokigib@rediffmail.com (A.K.)

<sup>4</sup> Shoolini University, Post Box No. 9, Head Post Office, Solan, H.P. 173212, India; Director, Amity University, Haryana (D.K.)

\* Correspondence: chatantadk@yahoo.com (D.K.); ashokigib@rediffmail.com (A.K.)

Scopus Author ID 57203256288

Received: 28.01.2022; Accepted: 8.03.2022; Published: 29.03.2022

**Abstract:** A simple and rapid nanocomposite-based immunosensor is proposed for diagnosing celiac disease. The disease is highly prevalent, and the average prevalence of the disease has been reported to be between 0.5 and 1% worldwide. The advantage of the developed method is that it is more sensitive and specific for detecting anti-gliadin antibodies elicited in response to gluten ingestion in celiac susceptible individuals. The antigen (gliadin) was immobilized onto the nanocomposite electrode, and subsequently, specific antibodies from the human serum samples were electrochemically detected using 50mM of  $K_3Fe(CN)_6$ . Cyclic Voltammetry (CV) and Differential Pulse Voltammetry (DPV) studies were carried out to record the electrochemical response. The modifications at each fabrication step were checked using Field emission-Scanning Electron Microscopy (FE-SEM). The sensor was specific and showed minimal response to non-specific serum proteins. The sensitivity and lower limit of detection of the developed sensor were  $762.6\mu A cm^{-2}ng^{-1}$  and 0.2pg per  $6\mu l$ , respectively.

**Keywords:** Celiac disease; gluten; immunosensor; nanocomposite; electrochemical immunosensor.

© 2022 by the authors. This article is an open-access article distributed under the terms and conditions of the Creative Commons Attribution (CC BY) license (<https://creativecommons.org/licenses/by/4.0/>).

## 1. Introduction

Celiac Disease (CD) is an intestinal disorder triggered by an inappropriate immune response to gluten and similar proteins of barley and rye in genetically susceptible individuals [1]. The prevalence of the disease is reported to be between 0.5 and 1% worldwide [1, 2]. However, it is suggested that CD is higher in patients with genetic and autoimmune diseases than in healthy individuals. The major triggering factors in CD are gliadins [2], which are deamidated by an enzyme tissue transglutaminase (tTG), resulting in an elevated immunostimulatory potential. When presented with human leukocyte antigens (HLA) DQ2 and DQ8 of antigen-presenting cells to CD4+ T cells, the deamidated peptides result in problems related to malabsorption [3, 4]. The serological changes involve the emergence of antibodies against gliadin, and tTG, the specific disease indicators. CD has varied symptoms; however, they all are non-specific; therefore, many CD patients are misdiagnosed with other diseases [5]. CD has a

high prevalence (about 1 %) worldwide [6], and its frequency is increasing, not only because the success rate of diagnosis is improving but also by the areal spread of the disease [7, 8]. Despite the various therapeutic strategies developed so far [9], the only way to treat this problem is to strictly follow a gluten-free diet [10].

Therefore, it is extremely important to diagnose CD early to control the gastrointestinal damage. The available tests for diagnosing CD include serological tests and biopsy of small bowel portion. Enzyme-linked immunosorbent assay (ELISA) has been routinely used for the detection of CD biomarkers [11-13]. However, it has various limitations in view of sensitivity, specificity, cost, and requirement of sophisticated instrumentation. Therefore, biosensors came out as a solution due to their higher sensitivity and specificity, lower sample volumes requirement, and short analysis time [14-18].

Various electrochemical immunosensors have been employed for detecting antibodies in celiac susceptible individuals [19-34]. However, these methods are less sensitive and specific for antibody detection. Hence, in the present study, a multi-walled carbon nanotubes-gold nanoparticles (MWCNT/AuNP)-Mercaptopropionic acid (MPA)-polyamidoamine (PAMAM) composite based electrochemical immunosensor was proposed for detecting anti-gliadin antibodies in human serum to aid in point-of-care analysis. MWCNT/AuNP platform in the electrode was used to increase the surface area, thereby leading to enhanced sensitivity. PAMAM is used in electrochemical biosensors due to its branched (tree-like) polymeric structures that contain a large number of amino groups for conjugation with desired carboxylated probes, and MPA is used for the activation of the thiol group of gold nanoparticles.

## 2. Materials and Methods

### 2.1. Materials.

Polyamidoamine (PAMAM) dendrimer third-generation (G3; Mol. Wt.-6909), 1-Ethyl-3-(3-dimethyl-aminopropyl) carbodiimide (EDC) and N- hydroxysuccinimide (NHS), anti-gliadin (wheat) antibody, Potassium ferricyanide (K<sub>3</sub>Fe (CN)<sub>6</sub>) were procured from Sigma- Aldrich, USA. Hydrogen peroxide (H<sub>2</sub>O<sub>2</sub>), sodium chloride (NaCl), potassium chloride (KCl), disodium hydrogen phosphate (Na<sub>2</sub>HPO<sub>4</sub>), potassium dihydrogen phosphate (KH<sub>2</sub>PO<sub>4</sub>), ethanol, and other chemicals were obtained from Qualigens, India. ELISA kit specific for gliadin IgG isotype was procured from Diagnostics and Scientific Suppliers, Chandigarh, India.

Screen printed Multi-walled Carbon Nanotubes-gold nanoparticles (MWCNT/AuNP) electrodes. A specific connector was purchased from DropSend, Spain, and modified at the Institute of Genomics and Integrative Biology (IGIB), New Delhi, India. The serum samples for carrying out the study were procured from Health Centre, Shoolini University, Solan, India.

### 2.2. Fabrication of the MWCNT/AuNP-MPA-PAMAM composite.

For fabricating the immunosensor, a screen-printed electrode (MWCNT/AuNP) was used. It was first washed with autoclaved distilled water, followed by dehydration with ethanol. The working electrode surface was then modified by adding MPA(6 $\mu$ l). This was followed by washing to remove unbound MPA and finally drying at room temperature.

The COOH groups on the surface were activated by treating the carboxylated electrode with an equimolar mixture of a cross-linking agent, EDC, and NHS (10 mM, 1:1, v/v) prepared in 50 mM PBS for 1 h. 6 $\mu$ l of PAMAM was then incubated onto the working surface for 6 h. After the reaction, the electrode was again washed and dried at room temperature.

### 2.3. Immobilization of gliadin (antigen).

The activation of the COOH assembly on the antigen was done by mixing 3 $\mu$ l of 2mg/ml gliadin with 3 $\mu$ l of EDC and NHS (10 mM each) for making the final antigen concentration 1mg/ml. This mixture was then incubated overnight on the working surface at 4°C to allow the amide bond formation between the antigen and PAMAM to make MWCNT/AuNP–MPA–PAMAM–antigen electrode. To remove the unbound antigen, washing was then done, followed by drying at room temperature before electrochemical detection.

### 2.4. Hybridization with anti-gliadin antibodies.

The MWCNT/AuNP-MPA-PAMAM-antigen electrode was hybridized with 0.001, 0.01, 0.1, 10,100, and 1000ng per 6 $\mu$ l anti-gliadin antibody in human serum for 10 min on the surface of the working electrode. After hybridization, the electrode surface was first washed with tween 20 (3-4 times). With PBS (pH 7), followed by drying at room temperature before electrochemical analysis was done using  $K_3Fe(CN)_6$ , which acts as the redox indicator.

### 2.5. FE-SEM analysis.

Field Emission Scanning electron microscopy (FE-SEM, Hitachi,4300, SE/N) studies were performed to analyze the changes in electrode surface morphology at different fabrication stages. The modified screen-printed electrodes were coated with gold (6 nm thickness) using a sputter coater under a vacuum and were scanned under a scanning electron microscope. The images of different modifications were then observed.

### 2.6. Precision and accuracy studies.

To check the accuracy of the present method, gliadin IgG antibodies ELISA was carried out with an anti-gliadin antibody in serum. Different antibody concentrations viz. 0 (control), 0.1, 0.5, 1, 2, 5, and 10ng per ml prepared in serum were incubated with gliadin immobilized on the microtitre plate (96 wells). After 30 min of incubation, the wells were washed using a washing buffer.

After that, horseradish peroxidase-labeled rabbit anti-human IgG that binds to surface-bound antibodies was added to the well during incubation of 30 min. Washing was done to remove the unbound conjugate. After that, the solution containing TMB reagent and enzyme-substrate was added to monitor specific antibody binding. Stop solution was then added to stop the reaction and provide appropriate pH for color development. The optical densities (absorbance) were then measured using a microplate reader at 450nm.

### 2.7. Statistical Analysis.

Means, Standard deviation, slope, regression analysis was calculated using Microsoft Excel 2007.

## 3. Results and Discussion

The fabrication and electrochemical detection of the composite electrode, from immobilizing gliadin to hybridizing with anti-gliadin antibodies to form MWCNT/AuNP–MPA–PAMAM/antigen/antibody, is shown diagrammatically in Figure 1.

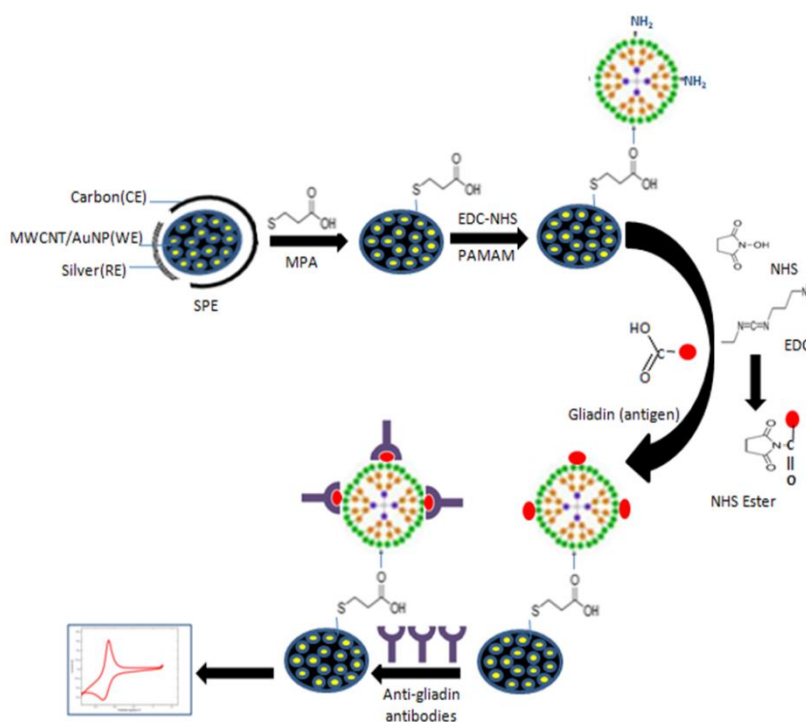


**Figure 1.** Schematic fabrication of the MWCNT/AuNP–MPA–PAMAM composite electrode, immobilization of antigen, gliadin, and hybridization with anti-gliadin antibodies to form MWCNT/AuNP–MPA–PAMAM/antigen/antibody and its electrochemical detection. SPE: Screen-Printed Electrode (CE: Counter Electrode, WE: Working Electrode, RE: Reference Electrode).

### 3.1. Electrochemical studies for detecting anti-gliadin antibodies on nanohybrid electrode immobilized with antigen.

Various electrochemical immunosensors have been employed for detecting specific antigens/antibodies in celiac susceptible individuals. However, these methods are less sensitive and specific for analyte detection. In the present study, the electrochemical response was recorded in the form of CV and DPV. It was observed that when anti-gliadin antibodies were absent, a high current response was seen in the nanohybrid electrode with antigen (gliadin). However, a decrease in current response was recorded in the presence of anti-gliadin antibodies. The reduction in current with increasing concentrations of anti-gliadin antibodies was due to the formation of an additional immune layer on the electrode surface at each step of fabrication.

### 3.2. CV studies.

Potassium ferricyanide was used to carry out the CV measurements of immobilized antigen and hybridization with antibody. The peak current ( $I_p$ ) of the probe (MWCNT/AuNP/MPA/PAMAM/gliadin/serum) was used as a control for different concentrations of antibodies that were prepared in human serum (Figure 2). The  $I_p$  of antibody hybridized electrode was found to be lower than that of antigen. An inverse relation was observed between  $I_p$  and increasing concentrations of antibodies through the successive immune-complex formation.

A hyperbolic curve was observed between various concentrations of antibody and the relative  $I_p$  values with reference to the probe (Figure 2, inset A) following a linear equation [ $I_p$  ( $\mu\text{A}$ ) =  $85.58$  ( $\mu\text{A ng}^{-1}$ )  $\times$  anti-gliadin antibody (ng) +  $7.5$ ] and regression coefficient ( $R^2$ )  $0.983$  (Fig 2, inset B). The sensitivity (S) was calculated using the formula,  $S = m/A$ , where ‘m’ and

'A' correspond to the slope and area of the working (0.126 cm<sup>2</sup>) electrode surface, respectively, was found to be 679.2 μA cm<sup>-2</sup>ng<sup>-1</sup>. The limit of detection (LOD) for anti-gliadin antibody was found to be 0.2pg per 6μl, which was calculated using LOD = 3 (s/S), where s is the standard deviation and S is the sensitivity [35-37].

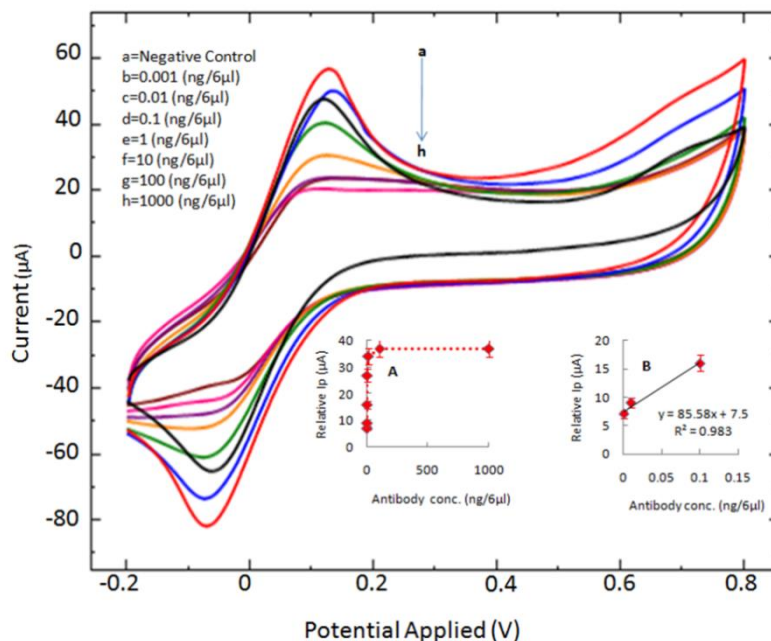


**Figure 2.** Cyclic voltammetric studies of gliadin immobilized nano hybrid electrode hybridized with 0.001ng/6μl to 1000ng/6μl anti-gliadin antibody in serum (a→h) using 5mM K<sub>3</sub>Fe(CN)<sub>6</sub> in 0.1M PBS, pH 7.4. Inset A shows a hyperbolic curve between relative Ip (with respect to control) and increasing concentrations of anti-gliadin antibodies ranging from 0.001-1000ng/6μl in serum. Inset B shows the linear plot from 0.001-0.1ng/6μl anti-gliadin antibodies to calculate sensitivity and LOD.

### 3.3. DPV studies.

In DPV measurements, similar patterns of peak current were observed (Figure 3) as in CV measurements.

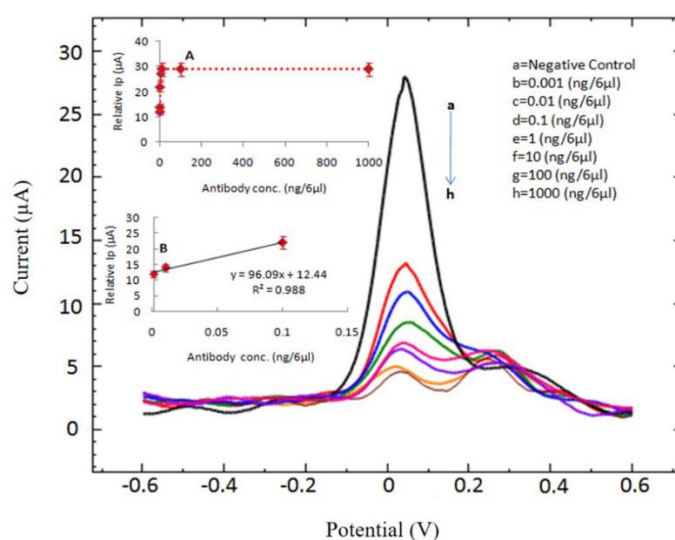


**Figure 3.** Differential Pulse voltammetric studies of gliadin immobilized nano hybrid electrode hybridized with 0.001ng/6μl to 1000ng/6μl anti-gliadin antibody in serum (a→h) using 5mM K<sub>3</sub>Fe(CN)<sub>6</sub> in 0.1M PBS, pH 7.4. Inset A shows a hyperbolic curve between relative Ip (with respect to control) and increasing concentrations of anti-gliadin antibodies ranging from 0.001-1000ng/6μl in serum. Inset B shows the linear plot from 0.001-0.1ng/6μl anti-gliadin antibodies for the calculation of sensitivity and LOD.

With an increase in the concentrations of antibodies, a reduction in peak current was observed. A hyperbolic curve was observed between different antibody concentrations and the relative  $I_p$  values with respect to the probe (Fig 3, inset A) following the linear equation [ $I_p$  ( $\mu\text{A}$ ) =  $96.09$  ( $\mu\text{A ng}^{-1}$ )  $\times$  anti-gliadin antibody (ng) +  $12.44$ ] and regression coefficient ( $R^2$ ) was  $0.988$  (Figure 3, inset B). The sensor's sensitivity was  $762.6\mu\text{A cm}^{-2}\text{ng}^{-1}$ , and LOD was found to be  $0.2\text{pg}/6\mu\text{l}$ .

### 3.4. FE-SEM analysis.

The different stages of fabrication of the composite electrode (Figure 4) were studied using field emission-scanning electron microscopy (FE-SEM).

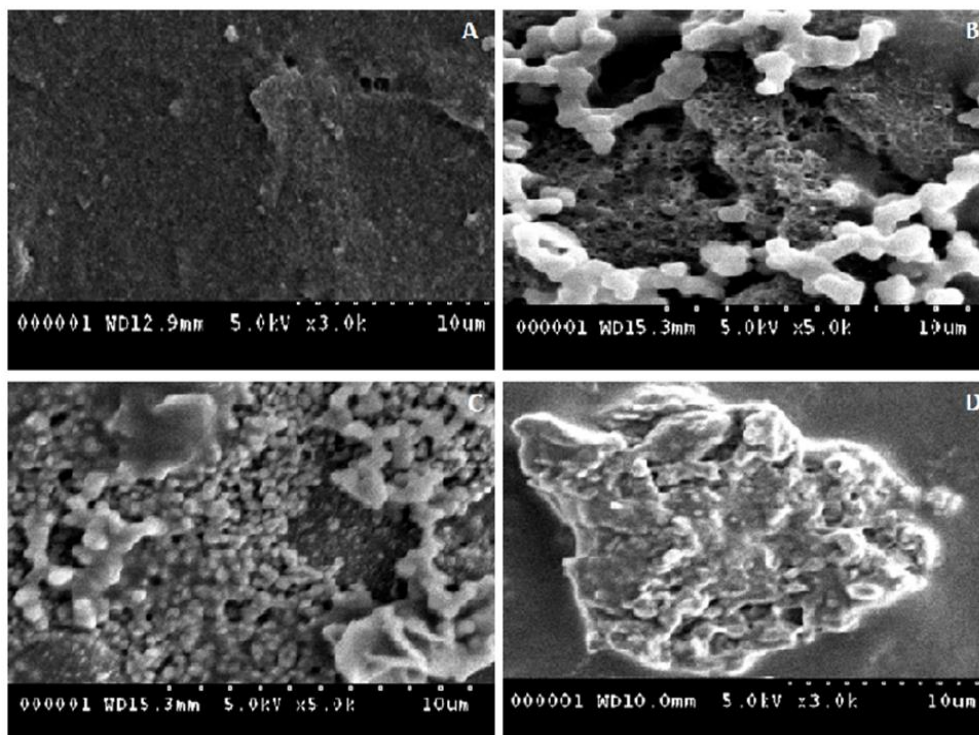


**Figure 4.** FE-SEM scans of (A) MWCNT/AuNP/MPA, (B) MWCNT/AuNP/MPA/PAMAM, (C) MWCNT/AuNP/MPA/PAMAM/Gliadin and (D) MWCNT/AuNP/MPA/PAMAM/Gliadin/anti-gliadin antibody composite electrodes.

The FE-SEM image of the MWNT/AuNP electrode with mercaptopropionic acid (MPA) in Figure 4A exhibits a smooth and uniform structure [38]. A significant change in surface morphology in terms of branched structures was observed when PAMAM was added onto the MPA fabricated electrode surface (Figure 4B). Figure 4C shows MWCNT/Au-MPA-PAMAM/gliadin exhibiting scattered structures, and Figure 4D shows MWCNT/Au-MPA-PAMAM/gliadin/anti-gliadin antibody.

The MWCNT/Au-MPA-PAMAM/gliadin/anti-gliadin antibody is denser in surface morphology than the MWCNT/Au-MPA-PAMAM/gliadin, which confirms the hybridization of the antigen with the antibody.

### 3.5. Specificity, sensitivity, and stability of the sensor.

The specificity of the sensor was evaluated via DPV measurements with anti-gliadin antibody and various proteins found in serum like Creatinine, Cardiac Troponin I, human serum albumin, and Cystatin C. The DPV peak current ( $I_p$ ) of the sensor after incubation with different

serum proteins (1 ng per 6μl) for 10 min each were found to be almost similar to the probe (Figure 5).

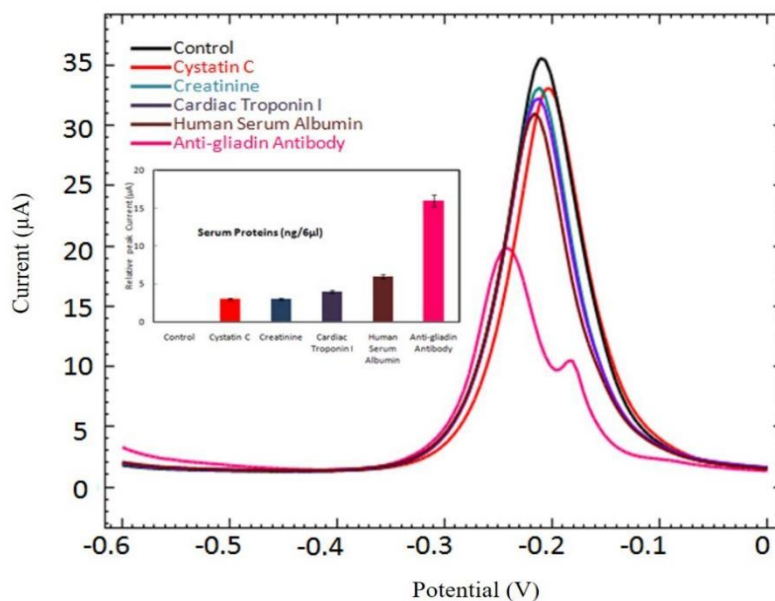


**Figure 5.** The specificity MWCNT/AuNP/MPA/PAMAM/Gliadin sensor with anti-gliadin antibody and other serum proteins. The inset shows the average relative Ip value of DPV (with respect to control incubated in serum) after hybridization with specific and non-specific serum proteins (1ng/6μl).

A significant reduction in Ip was recorded only with antibody, confirming the sensor’s specificity to the anti-gliadin antibody. The bar graph of relative peak current with anti-gliadin antibody and different serum proteins is shown in the inset. The stability of the electrode immobilized with the probe was evaluated by determining the change in the DPV peak current every 30 days of storage at 4°C. The developed sensor was found stable for 6 months at 4°C with just a 10% decrease in the initial Ip of the immobilized probe.

### 3.6. Precision and accuracy studies.

The accuracy of the present method was checked by ELISA kit (y-axis) and compared with those determined by the present MWCNT/Au–MPA–PAMAM based nanohybrid sensor (x-axis).

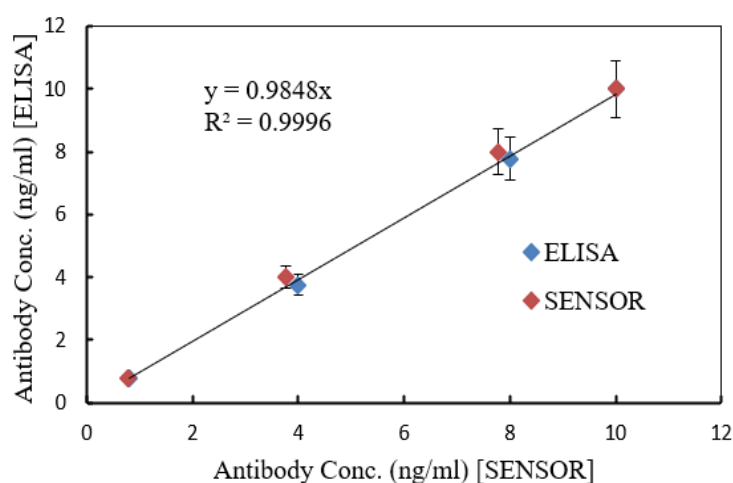


**Figure 6.** Determination of accuracy of the present method (x-axis) and ELISA kit method (y-axis).

The unknown concentrations of antigliadin antibody (0.8, 4, 8, and 10ng/ml in serum) were made, and real values obtained by both methods (ELISA and Immunosensor) from the standard curve were plotted (Figure 6), which showed a good correlation ( $R^2=0.998$ ) with linear equation ( $y=0.984x$ ).

#### 4. Conclusions

A simple and rapid nanocomposite-based immunosensor has been developed to diagnose celiac disease. The analytical parameters of the optimized immunosensor based method can detect as low as 0.2pg per 6 $\mu$ l (35.8pg per ml) anti-gliadin antibodies in 10 min, confirming the sensor's sensitivity.

#### Funding

This research received no external funding.

#### Acknowledgments

The research is supported by Shoolini University, Solan (H.P.), and IGIB, Delhi.

#### Conflicts of Interest

The authors declare no conflict of interest.

#### References

1. Sahin, Y. Celiac disease in children: A review of the literature. *World journal of clinical pediatrics* **2021**, *10*, 53-71, <https://doi.org/10.5409/wjcp.v10.i4.53>.
2. Barone, M.V.; Auricchio, S.A. Cumulative Effect of Food and Viruses to Trigger Celiac Disease (CD): A Commentary on the Recent Literature. *Int J Mol Sci* **2021**, *22*, 2027, <https://doi.org/10.3390/ijms22042027>.
3. Sánchez, D.; Hoffmanová, I.; Szczepanková, A.; Hábová, V.; Tlaskalová-Hogenová, H. Contribution of Infectious Agents to the Development of Celiac Disease. *Microorganisms* **2021**, *9*, 547, <https://doi.org/10.3390/microorganisms9030547>.
4. Galipeau, H.J.; Verdu, E.F. The double-edged sword of gut bacteria in celiac disease and implications for therapeutic potential. *Mucosal Immunol* **2022**, 1-9, <https://doi.org/10.1038/s41385-021-00479-3>.
5. Pasinszki, T.; Krebsz, M. Biosensors for Non-Invasive Detection of Celiac Disease Biomarkers in Body Fluids. *Biosensors* **2018**, *8*, 55, <https://doi.org/10.3390/bios8020055>.
6. Akbari Namvar, Z.; Mahdavi, R.; Shirmohammadi, M.; Nikniaz, Z. The effect of group-based education on gastrointestinal symptoms and quality of life in patients with celiac disease: randomized controlled clinical trial. *BMC Gastroenterol* **2022**, *22*, 18, <https://doi.org/10.1186/s12876-022-02096-1>.
7. Scherf, K.A.; Ciccocioppo, R.; Pohanka, M.; Rimarova, K.; Opatrilova, R.; Rodrigo, L.; Kruzliak, P. Biosensors for the Diagnosis of Celiac Disease: Current Status and Future Perspectives. *Mol Biotechnol* **2016**, *58*, 381–392, <https://doi.org/10.1007/s12033-016-9940-3>.
8. Samasca, G.; Lerner, A. Celiac disease in the COVID-19 pandemic. *J Transl Autoimmun* **2021**, *4*, 100120, <https://doi.org/10.1016/j.jtauto.2021.100120>.
9. Sollid, L.M.; Khosla, C. Future therapeutic options for celiac disease. *Nat Rev Gastroenterol Hepatol* **2005**, *2*, 140–147, <https://doi.org/10.1038/ncpgasthep0111>.
10. Pinto-Sanchez, M.I.; Silvester, J.A.; Lebwohl, B.; Leffler, D.A.; Anderson, R.P.; Therrien, A.; Kelly, C.P.; Elena F.V. Society for the Study of Celiac Disease position statement on gaps and opportunities in coeliac disease. *Nat Rev Gastroenterol Hepatol* **2021**, *18*, 875–884, <https://doi.org/10.1038/s41575-021-00511-8>.
11. Teesalu, K.; Agardh, D.; Panarina, M.; Utt, M.; Uibo, O.; Uibo, R. A modified ELISA for improved detection of IgA, IgG, and IgM anti-tissue transglutaminase antibodies in celiac disease. *Clinica Chimica Acta* **2009**, *403*, 37–41, <https://doi.org/10.1016/j.cca.2009.01.006>.

12. Basso, D.; Guariso, G.; Bozzato, D.; Rossi, E.; Pescarin, M.; Fogar, P.; Moz, S.; Navaglia, F.; Peloso, M.; Gasparetto, M.; Zambon, C.F.; Padoan, A.; Greco, E.; Rugge, M.; Plebani, M. New screening tests enrich anti-transglutaminase results and support a highly sensitive two-test based strategy for celiac disease diagnosis. *Clinica Chimica Acta* **2011**, *412*, 1662–1667, <https://doi.org/10.1016/j.cca.2011.05.024>.
13. Horton, R.K.; Hagen, C.E.; Snyder, M.R. Pediatric Celiac Disease: A Review of Diagnostic Testing and Guideline Recommendations. *J Appl Lab Med* **2022**, *7*, 294–304, <https://doi.org/10.1093/jalm/jfab143>.
14. Wang, J. Electrochemical biosensors: Towards point-of-care cancer diagnostics. *Biosens Bioelectron* **2006**, *21*, 1887–1892, <https://doi.org/10.1016/j.bios.2005.10.027>.
15. Ronkainen, N.J.; Halsall, H.B.; Heineman, W.R. Electrochemical biosensors. *Chem Soc Rev* **2010**, *39*, 1747–1763, <https://doi.org/10.1039/b714449k>.
16. Neves, M.M.P.S.; González-García, M.B.; Nouws, H.P.A.; Costa-García, A. Celiac disease detection using a transglutaminase electrochemical immunosensor fabricated on nanohybrid screen-printed carbon electrodes. *Biosens Bioelectron* **2012**, *31*, 95–100, <https://doi.org/10.1016/j.bios.2011.09.044>.
17. Neves, M.M.P.S.; González-García, M.B.; Delerue-Matos, C.; Costa-García, A. Multiplexed electrochemical immunosensor for detection of celiac disease serological markers. *Sens Actuators B Chem* **2013**, *187*, 33–39, <https://doi.org/10.1016/j.snb.2012.09.019>.
18. Martín-Yerga, D.; Costa-García, A. Electrochemical Immunosensors for Celiac Disease Detection. *Int J Celiac Dis* **2016**, *2*, 139–141, <https://doi.org/10.12691/ijcd-2-4-1>.
19. Balkenhohl, T.; Lisdat, F. An impedimetric immunosensor for the detection of autoantibodies directed against gliadins. *Analyst* **2007**, *132*, 314, <https://doi.org/10.1039/b609832k>.
20. Balkenhohl, T.; Lisdat, F. Screen-printed electrodes as impedimetric immunosensors for the detection of anti-transglutaminase antibodies in human sera. *Analytica Chimica Acta* **2007**, *597*, 50–57, <https://doi.org/10.1016/j.aca.2007.06.04>.
21. Pividori, M.I.; Lermo, A.; Bonanni, A.; Alegret, S.; del Valle, M. Electrochemical immunosensor for the diagnosis of celiac disease. *Anal Biochem* **2009**, *388*, 229–234, <https://doi.org/10.1016/j.ab.2009.02.026>.
22. Pereira, S.V.; Raba, J.; Messina, G.A. IgG anti-gliadin determination with an immunological microfluidic system applied to the automated diagnostic of the celiac disease. *Anal Bioanal Chem* **2010**, *396*, 2921–2927, <https://doi.org/10.1007/s00216-010-3589-8>.
23. Ortiz, M.; Fragoso, A.; O’Sullivan, C.K. Detection of Antigliadin Autoantibodies in Celiac Patient Samples Using a Cyclodextrin-Based Supramolecular Biosensor. *Anal Chem* **2011**, *83*, 2931–2938, <https://doi.org/10.1021/ac102956p>.
24. Dulay, S.; Lozano-Sánchez, P.; Iwuoha, E.; Katakis, I.; O’Sullivan, C.K. Electrochemical detection of celiac disease-related anti-tissue transglutaminase antibodies using thiol-based surface chemistry. *Biosens Bioelectron* **2011**, *26*, 3852–3856, <https://doi.org/10.1016/j.bios.2011.02.04>.
25. Rosales-Rivera, L.C.; Acero-Sánchez, J.L.; Lozano-Sánchez, P.; Katakis, I.; O’Sullivan, C.K. Electrochemical immunosensor detection of antigliadin antibodies from real human serum. *Biosens Bioelectron* **2011**, *26*, 4471–4476, <https://doi.org/10.1016/j.bios.2011.05.004>.
26. Martín-Yerga, D.; Costa-García, A. Towards a blocking-free electrochemical immunosensing strategy for anti-transglutaminase antibodies using screen-printed electrodes. *Bioelectrochem* **2015**, *105*, 88–94, <https://doi.org/10.1016/j.bioelechem.2015.05.014>.
27. Longo, S.; De Leo, L.; Not, T.; Ugo, P. Nanoelectrode Ensemble Immunosensor Platform for the Anodic Detection of Anti-Tissue Transglutaminase Isotype IgA. *J. Electroanal. Chem* **2021**, 115984, <https://doi.org/10.1016/j.jelechem.2021.115984>.
28. Zhang, J.; Liu, W.; Gong, W.; Liu, N.; Jia, Y.; Ding, D.; Ning, Z. Ultrasensitive Determination of Microcystin-Leucine-Arginine (MCLR) by an Electrochemiluminescence (ECL) Immunosensor with Graphene Nanosheets as a Scaffold for Cadmium-Selenide Quantum Dots (QDs). *Anal. Lett.* **2021**, 1–14, <https://doi.org/10.1080/00032719.2021.1875479>.
29. Torre, R.; Freitas, M.; Costa-Rama, E.; Nouws, H.; Delerue-Matos, C. Tropomyosin Analysis in Foods Using an Electrochemical Immunosensing Approach. *Chem. Proc* **2021**, *5*, 62, <https://doi.org/10.3390/CSAC2021-10471>.
30. Bhakta, S.; Mishra, P. Molecularly imprinted polymer-based sensors for cancer biomarker detection. *Sensors and Actuators Reports* **2021**, *3*, 100061, <https://doi.org/10.1016/j.snr.2021.100061>.
31. Arrigan, D. W. Nanoelectrode arrays for electroanalysis. *Front. Nanosci* **2021**, *18*, 49–86, <https://doi.org/10.1016/B978-0-12-820055-1.00006-X>.

32. Koushki, K.; Keshavarz Shahbaz, S.; Keshavarz, M.; Bezsonov, E. E.; Sathyapalan, T.; Sahebkar, A. Gold nanoparticles: Multifaceted roles in the management of autoimmune disorders. *Biomolecules* **2021**, *11*, 1289, <https://doi.org/10.3390/biom11091289>.
33. Kholafazad-Kordasht, H.; Hasanzadeh, M.; Seidi, F. Smartphone based immunosensors as next generation of healthcare tools: Technical and analytical overview towards improvement of personalized medicine. *TrAC - Trends Anal. Chem.* **2021**, *145*, 116455, <https://doi.org/10.1016/j.trac.2021.116455>.
34. Jiang, D.; Sheng, K.; Jiang, H.; Wang, L. A biomimetic “intestinal microvillus” cell sensor based on 3D bioprinting for the detection of wheat allergen gliadin. *Bioelectrochem* **2021**, *142*, 107919, <https://doi.org/10.1016/j.bioelechem.2021.107919>.
35. Dash, S.K.; Sharma, M.; Khare, S.; Kumar, A. rmpM Genosensor for Detection of Human Brain Bacterial Meningitis in Cerebrospinal Fluid. *Appl Biochem Biotechnol* **2013**, *171*, 198-208, <https://doi.org/10.1007/s12010-013-0339-3>.
36. Verma, V.; Kala, D.; Gupta, S.; Kumar, H.; Kaushal, A.; Kuća, K.; Cruz-Martins, N.; Kumar, D. Leptospira interrogans Outer Membrane Protein-Based Nanohybrid Sensor for the Diagnosis of Leptospirosis. *Sensors* **2021**, *7*, 2552, <https://doi.org/10.3390/s21072552>.
37. Kala, D.; Sharma, T.K.; Gupta, S.; Verma, V.; Thakur, A.; Kaushal, A.; Trukhanov, A.V.; Trukhanov, S.V. Graphene Oxide Nanoparticles Modified Paper Electrode as a Biosensing Platform for Detection of the htrA Gene of *O. tsutsugamushi*. *Sensors* **2021**, *21*, 4366, <https://doi.org/10.3390/s21134366>.
38. Dash, S.K.; Sharma, M.; Khare, S.; Kumar, A. Omp85 genosensor for detection of human brain bacterial meningitis. *Biotechnol Lett* **2013**, *35*, 929–935, <https://doi.org/10.1007/s10529-013-1161-2>.